Asian Journal of Chemistry; Vol. 26, No. 24 (2014), 0000-0000

ASIAN JOURNAL OF CHEMISTRY

Preparation and Properties of Novel Magnetic *Rhizopus oryzae* Biomass Particles for Removal of Anionic Azo Dyes from Aqueous Solution

YONG-QIAN FU*, HUAYUE ZHU, LONGFEI YIN, RU JIANG and XIN LI

Institute of Biomass Resources, Key Laboratory of Plant Evolutionary Ecology and Conservation, Taizhou University, Jiaojiang 318000, Zhejiang, P.R. China

*Corresponding author: Fax: +086 0576 8513 7066; Tel: +86 137 5063 3210; E-mail: fuyq@tzc.edu.cn; fuyongqian@sina.com

(*Received*: ; *Accepted*:) AJC-0000

Novel magnetic *Rhizopus oryzae* biomass particles (m-RBps) were prepared successfully and characterized by XRD, SEM and FT-IR. The ability of magnetic *Rhizopus oryzae* biomass particles to remove congo red from aqueous solutions has been carried out as a function of adsorbent dose (0.6-3 g/L), initial congo red concentration (5-80 mg/L) and contact time. An amount of 1 g/L of magnetic *Rhizopus oryzae* biomass particles could remove more than 95 % of the dye from 20 mg/L congo red solution. The amount of congo red adsorbed per unit weight of magnetic *Rhizopus oryzae* biomass particles increased from 6.3 to 65.19 mg with increasing concentration from 5 to 80 mg/L. In the kinetic study, the pseudo-second order kinetic model described the process of congo red adsorption on magnetic *Rhizopus oryzae* biomass particles at low congo red concentration (5-50 mg/L) very well. Adsorption kinetic studies also revealed that three stages in the adsorption process. Both film diffusion and intra-particle diffusion simultaneously operated during adsorption at low congo red concentrations (5-50 mg/L). Intra-particle diffusion is the sole rate-limiting step at high congo red concentration (80 mg/L). Isotherm modeling revealed that the Langmuir equation could better describe congo red adsorption on magnetic *Rhizopus oryzae* biomass particles compared with Freundlich models. The magnetic *Rhizopus oryzae* biomass particles may be a promising candidate of efficient, low cost, convenient separation under magnetic field.

Keywords: Biosorption, Congo red, Magnetic adsorbent, *Rhizopus oryzae*, Waste-water treatment.

INTRODUCTION

Textile industries discharge large amounts of colored wastewater containing various dyes (7,000,000 tons per year). Approximately 15 % of the total amount of dyes produced is lost during dyeing process and released as effluents[1,2]. The release of these dyes in water resources, even in small amounts, can affect aquatic life and the food web. Dyes can also cause allergic dermatitis and skin irritation and some of them have been reported to be carcinogenic and mutagenic to aquatic organisms and humans[3,4]. Thus, strong environmental regulations require that dye removal be performed before discharging wastewater into water bodies.

Treatment of dye effluents is difficult because these effluents are susceptible to oxidative catabolism and are generally non-biodegradable[5]. Only a few can be degraded microbiologically under anaerobic condition[6], but in most cases with the production of carcinogenic amines[7] and mutagens[8]. Several conventional procedures are available to remove dyes from wastewater, such as membrane separation, chemical oxidation, coagulation, flocculation and adsorption using different kinds of adsorbents[9-11]. Among these methods, adsorption is generally considered an effective method to quickly lower the concentration of dissolved dyes in effluents. Recently, different low-cost adsorbents including some industrial and agricultural wastes, such as fly ash, waste red mud, peat, rice husk, teakwood bark and so on, have been used to remove various dyes from wastewater[11-13]. However, their relatively low adsorption capacities or high costs towards to synthesized azo dyes limit practical application of these bioadsorbents. Therefore, new adsorbents must be developed to improve dye removal from wastewater.

Chitin, a (1→4)-linked *N*-acetyl-β-D-glucosamine, is a major polysaccharide found in crustaceous shells and in cell walls of fungi[14]. Chitin and its derivatives have been used as natural flocculants for anionic dye adsorption because amino and hydroxyl groups on their chains can serve as electrostatic interaction and coordination sites, respectively[15]. However, chitin is relatively expensive. Surface modification of chitin and its derivatives is considered a priority undertaking to improve the mechanical properties and specific gravity of chitin and further enhance its adsorption capacity for anionic dyes. Various studies[16-18] have been conducted to produce chitin

derivatives using chemical modification techniques. Although chitin modification products exhibit high adsorption capacity for dyes, they are inconvenient as adsorbents in practical applications because of their relative high cost and low specific gravity. Fungal biomass has a relatively high chitin content ranging[19,20] from 10 to 90 % and is considered to be a superior biosorbent for the removal of azo dyes[21,22]. However, fungi in the form of dispersed microorganisms has a small particle size, low density, poor mechanical strength and limited rigidity, like most biosorbents, thus causing practical difficulties in solid-liquid separation and biomass regeneration and limiting its application under real conditions[23,24].

Magnetic separation is a promising environmental purification technique because it produces no contaminants, such as flocculants and treats large amounts of wastewater within a short time period of time[25]. Magnetic nanoparticles embedded in porous polymer materials could expand the adsorption capacity of the matrix due to enhanced electrostatic interactions[26]. From the viewpoints of environmental protection and resource utilization, development of novel magnetic recyclable biomaterials, as well as exploration of their adsorption properties, is very important and significant to expand their utility as industrial biomaterials. Recently, magnetic chitin and its derivatives were obtained and applied in water treatment[27,28]. Magnetic microbial cells, such as *Saccharomyces cerevisiae*[29], *Kluyveromyces fragilis*[30], *Rhodopseudomonas spheroids*[31] and so on, have also been prepared and applied in dye removal. To the best of our knowledge, however, the characterization and adsorption properties of magnetic fungi biomass particles for dye removal have yet to be studied.

In the present study, novel magnetic *R. oryzae* biomass particles are prepared *via* a simple method and characterized using X-ray diffraction (XRD), scanning electron microscopy (SEM) and Fourier transform infrared spectroscopy (FT-IR). The effects of biosorbent dose, initial congo red concentration and contact time on the adsorption capacity of the anionic azo dye congo red on magnetic *Rhizopus oryzae* biomass particles are investigated. Models fitted to the equilibrium isotherm and kinetic data are presented to validate the usefulness of these novel magnetic *Rhizopus oryzae* biomass particles in the treatment of practical waste effluents.

EXPERIMENTAL

Congo red (molecular formula: $C_{32}H_{22}N_6Na_2O_6S_2$, molecular weight 696.66 g/mol), an anionic azo dye containing -NH_2 and -SO_3 functional groups, was selected as a model dye (Fig. 1). All solutions were prepared with double distilled water.

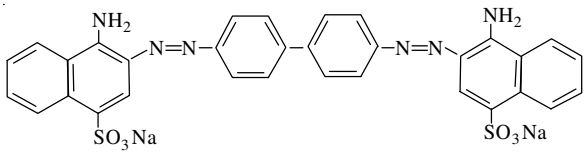

Fig. 1. Molecular structure of congo red

Preparation of *R. oryzae* biomass: The strain used was *R. oryzae* TZ-32, a mutant of *R. oryzae* ATCC 20344. The culture was routinely maintained at 4 °C on potato-dextrose agar (PDA) and aerobically cultivated in a nutrient broth containing (g/L): glucose 30, urea 2, KH_2PO_4 0.6, $MgSO_4·7H_2O$ 0.5, $ZnSO_4$ 0.11 and $FeSO_4·7H_2O$ 0.0088. The initial pH of the culture was adjusted from 5.5 to 6. The spores were incubated in a 250 mL shake flask containing 50 mL preculture medium at 200 rev/min and 30 °C for 24 h. The fully cultured biomass was harvested, filtered through a sieve and washed with double distilled water. The wet biomass was dried for 24 h at 60 °C in an oven. Dried biomass was powdered and collected for the following experiment.

Preparation of magnetic *Rhizopus oryzae* biomass particles: Approximately 4.08 g of $FeSO_4·7H_2O$ and 8.72 g of $FeCl_3·6H_2O$ (molar ratio of 1:2) were dissolved into 200 mL of deoxygenated distilled water, after which 10 g of powdered *R. oryzae* biomass was dispersed into the mixed iron salts. Chemical precipitation was achieved at 30 °C under 0.5 h of vigorous stirring by addition of 40 mL of $NH_3·H_2O$ solution (28 %, v/v) to the mixture in the presence of N_2. The reaction system was first heated at 40 °C for 20 min and then at 60 °C for 2 h. The system was then cooled to room temperature and pH was regulated to neutral. Precipitates were separated using an adscititious magnet, washed three times with ethanol and deoxygenated distilled water, respectively and then finally dried in an oven at 60 °C. Dried precipitates were powdered to obtain magnetic *Rhizopus oryzae* biomass particles.

Characterization of magnetic *Rhizopus oryzae* biomass particles: Wide-angle X-ray diffraction (XRD) measurements were carried out on an XRD diffractometer (D8-Advance, Bruker, USA). Samples were cut into powders in order to eliminate the influence from crystalline orientation. Patterns were obtained with CuK_α radiation ($\lambda = 0.15406$ nm) at 40 kV and 40 mA and recorded in the region of 2θ from 10 to 70° with a step speed of 2° min^{-1}. *R. oryzae* biomass and magnetic *Rhizopus oryzae* biomass particles surfaces were examined by SEM (Hitachi S4300). Materials were coated with platinum under vacuum conditions before the SEM experiments. The FT-IR spectra of the native and congo red laden magnetic *Rhizopus oryzae* biomass particles were obtained using a Thermo Nicolet NEXUS TM spectrophotometer. All samples were prepared as potassium bromide pellets.

Adsorption experiments: All batch adsorption experiments were performed on a shaking thermostat (KYC-1102C, Ningbo, China) with a constant speed of 100 rpm. Typically, 50 mL of a dye solution of a desired concentration and magnetic *Rhizopus oryzae* biomass particles with a desired dosage were added into 250 mL conical glass flasks with a constant speed of 100 rpm at 298 K. After the completion of preset time intervals, 5 mL of the dispersion was drawn and separated immediately using an adscititious magnet to collect the bioadsorbent. The residual congo red concentration in the supernate was analyzed at $\lambda_{max} = 496$ nm using a Cary 50 model UV-visible spectrophotometer (Varian, USA). The concentration retained in the adsorbent phase (q_t, mg/g) and color removal efficiency (η, %) were calculated using eqns. 1-2, respectively.

$$q_t = \frac{(C_0 - C_t)V}{W} \quad (1)$$

$$\eta(\%) = \frac{(C_0 - C_t)}{C_0} \times 100\ \% \quad (2)$$

where C_0(mg/L) is the initial congo red concentration and C_t (mg/L) is the congo red concentration at time t (min), V (l) is the volume of solution and W (g) is the bioadsorbent weight.

RESULTS AND DISCUSSION

XRD analysis: Fig. 2 shows the XRD patterns of (a) the *R. oryzae* biomass, (b) Fe_3O_4 and (c) the magnetic *Rhizopus oryzae* biomass particles. The wide and irregular peak illustrated that the *R. oryzae* biomass is not a single crystal structure, but of mixed composition. The main peak at $2\theta = 19.73°$ is assigned to the (110) planes similar to that of chitin and its derivatives. Thus, chitin may be the main component of *R. oryzae* biomass[14,15,32]. The main peaks of Fe_3O_4 were at 30.32, 35.64, 43.36, 53.67, 57.26 and 62.87°, r espectively corresponded to the (2 2 0), (3 1 1), (4 0 0), (4 2 2), (5 1 1) and (4 4 0) crystal planes of pure Fe_3O_4 with a spinal structure[28]. In the XRD pattern of the magnetic *Rhizopus oryzae* biomass particles, six obvious diffraction peaks of (2 2 0), (3 1 1), (4 0 0), (4 2 2), (5 1 1) and (4 4 0) were observed, indicating the introduction of Fe_3O_4 with a spinal structure into the magnetic *Rhizopus oryzae* biomass particles surfaces. The diffraction peak of *R. oryzae* at $2\theta = 19.73°$ could not be found in XRD pattern of the magnetic *Rhizopus oryzae* biomass particles, indicating that a change in the structure of chitin occurred preparation.

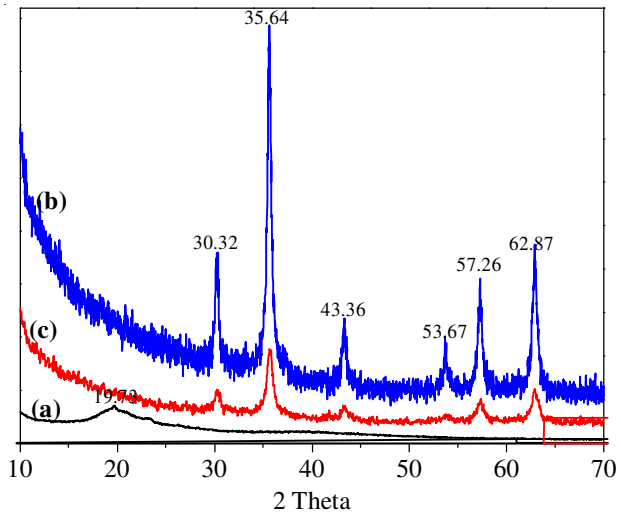

Fig.2. X-ray powder diffraction patterns for (a) *R. oryzae* biomass, (b) Fe_3O_4 and (c) magnetic *Rhizopus oryzae* biomass particles

SEM analysis: SEM is used extensively as a tool for biosorbent characterization[33]. A comparison between the SEM images of the *R. oryzae* biomass and those of the magnetic *Rhizopus oryzae* biomass particles is illustrated in Fig. 3. The surface morphology of pristine *R. oryzae* biomass is conspicuously different from that of the magnetic *Rhizopus oryzae* biomass particles. Magnified images of *R. oryzae* biomass show a smooth and homogeneous surface morphology (Fig. 3a,b). No obvious pores and voids were found on the *R. oryzae* biomass surface, indicating it's relatively dense. In contrast, magnetic *Rhizopus oryzae* biomass particles surface clearly turned rough and irregular when Fe_3O_4 particles were attached to them (Fig. 3c,d). Obviously, the uneven surface of the magnetic *Rhizopus oryzae* biomass particles indicated active adsorption sites and provides an advantageous condition for attracting more target pollutants around the sites. Thus, improved adsorption rates and capacities could be expected from the magnetic *Rhizopus oryzae* biomass particles[34].

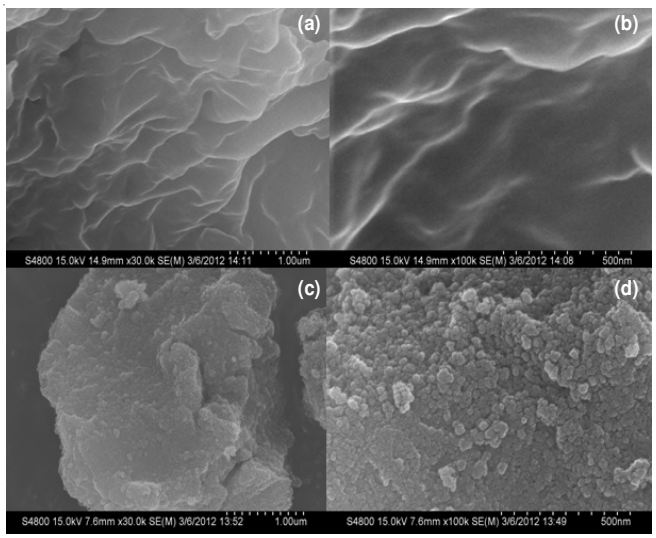

Fig. 3. SEM images for (a-b) *R. oryzae* biomass particle and (c-d) magnetic *Rhizopus oryzae* biomass particles

Magnetic recovery of magnetic *Rhizopus oryzae* biomass particles: The prepared magnetic *Rhizopus oryzae* biomass particles could be readily dispersed in water under stirring (Fig. 4a).

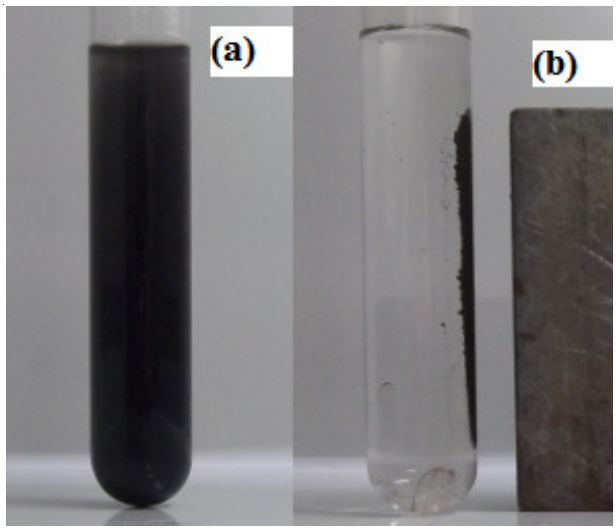

Fig. 4. Photographs of (a) magnetic *Rhizopus oryzae* biomass particles dispersed in treated water solution and (b) magnetic *Rhizopus oryzae* biomass particles by an ordinary magnet after 5 s

Moreover, the magnetic *Rhizopus oryzae* biomass particles could be easily separated from the treated solution and collected at the sidewalls of a cuvette after 5s using an ordinary magnet (Fig. 4b), suggesting the excellent magnetic responsivity of the prepared magnetic *Rhizopus oryzae* biomass particles. Magnetic responsivity is necessary for the magnetic separation and recovery of magnetic *Rhizopus oryzae* biomass particles from dye-containing effluents.

FT-IR analysis: The FT-IR spectra of magnetic *Rhizopus oryzae* biomass particles before and after congo red biosorption were taken from 4000-400 cm^{-1} to identify active functional groups during biosorption as shown in Fig. 5.

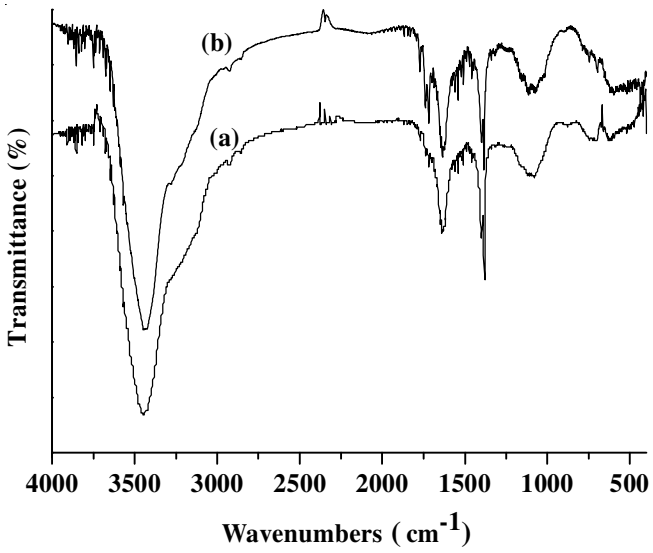

Fig. 5. FT-IR spectra of magnetic *Rhizopus oryzae* biomass particles: (a) before congo red biosorption; (b) after congo red biosorption

A strong band at 3450 cm^{-1} reflected N-H and O-H stretching vibrations of hydroxyl and amine groups on the surface of the magnetic *Rhizopus oryzae* biomass particles. The band at 2930 cm^{-1} could be due to the asymmetric vibrations of CH_2. The band at 1728 cm^{-1} could be ascribed to the carboxyl groups of amino acids. A distinct band at 1640 cm^{-1} resulted from the stretching vibrations of the CO and CN (amide I) peptidic bonds of proteins. The signal located near 1384 cm^{-1} is due to the (amide III) band. A strong band around 1100-1000 cm^{-1} corresponds to the C-O bond, which is the characteristic peak of polysaccharides[35-37].

All band intensities at 1640 (amide I) and 1384 cm^{-1} (amide III) clearly decreased after congo red biosorption, indicating an interaction between congo red and the amine groups of proteins. Bands at 1640 and 1384 cm^{-1} also shifted to 1635 and 1380 cm-1, respectively. After loading magnetic *Rhizopus oryzae* biomass particles with congo red, band intensities at 3450, 2930, 1728 and 1080 cm^{-1} all decreased. In addition, bands at 3450, 2930, 1728 and 1080 cm^{-1} shifted to 3435, 2925, 1718 and 1074 cm^{-1}, respectively. These changes in FT-IR spectra suggest the involvement of NH and OH of hydroxyl and amine groups, the CH_2 group of lipids, carboxyl groups of amino acids and the CO group of polysaccharides in congo red biosorption on magnetic *Rhizopus oryzae* biomass particles.

Effects of magnetic *Rhizopus oryzae* biomass particles dose: The effects of magnetic *Rhizopus oryzae* biomass particles dosage were studied on congo red removal from aqueous solutions with various magnetic *Rhizopus oryzae* biomass particles amounts from 0.6 to 3.0 g L^{-1} at a fixed initial concentration of 20 mg L^{-1}. The result is shown in Fig. 6.

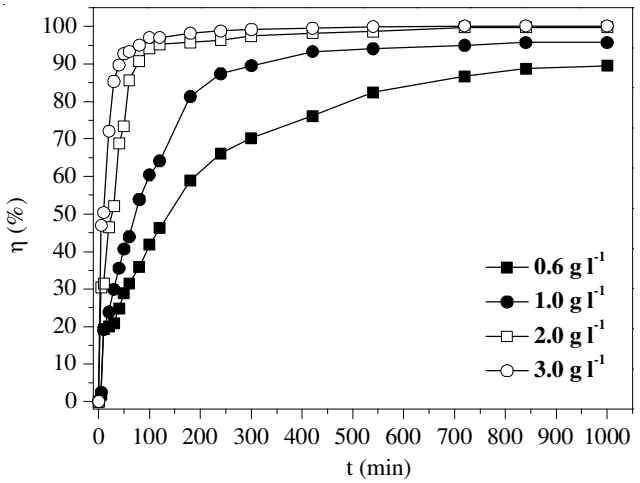

Fig. 6. Effect of adsorbent dosage on the removal of congo red (T = 298K; initial congo red concentration = 20 mg L^{-1}; shaking speed = 100 rpm)

An increase in the adsorbent dosage could increase the percentage of congo red removal from the solution. With increasing adsorbent dosage, more surface area was available for adsorption due to the increase in active sites on the surface of the magnetic *Rhizopus oryzae* biomass particles, thus allowing easier penetration of congo red ions into the sorption sites[38]. In contrast, however, the congo red uptake capacity (q_e) decreased with increasing magnetic *Rhizopus oryzae* biomass particles dosage due to splitting effects of the flux (concentration gradient) between the adsorbate and adsorbent[39]. Based on the results obtained, further studies on adsorption equilibrium study were conducted using 1 g/L magnetic *Rhizopus oryzae* biomass particles.

Effects of initial congo red concentration and contact time: The removal of congo red with different initial concentrations as a function of contact time was studied, the results of which are shown in Fig. 7.

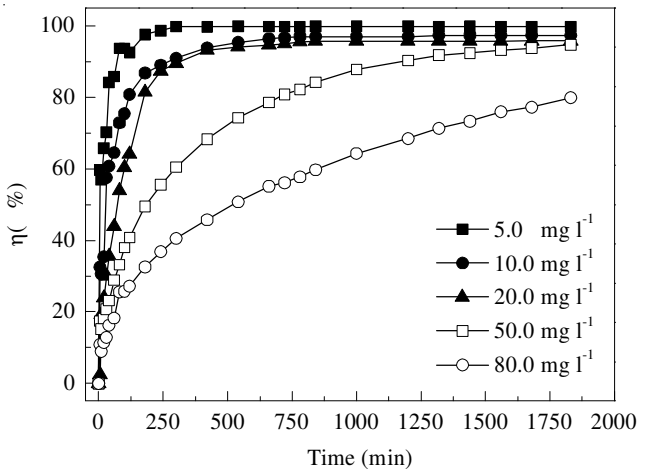

Fig. 7. Effect of initial concentrations on the removal of congo red onto magnetic *Rhizopus oryzae* biomass particles (T = 298 K; adsorbent dosage = 1.0 g L^{-1}; shaking speed = 100 rpm)

The color removal efficiency of magnetic *Rhizopus oryzae* biomass particles rapidly increased initially and then slowed down gradually until equilibrium was attained at low initial concentrations (5-20 mg L^{-1}). Approximately, 92.6, 80.8 and

64.1 % removal were observed within 2 h and the final color removal was found to be as high as 99.8, 97.1 and 95.5 % within 5, 12 and 13 h, respectively. As the congo red initial concentration increased (50-80 mg L^{-1}), the color removal efficiency of congo red solution onto magnetic *Rhizopus oryzae* biomass particles by adsorption slowly increased until equilibrium was attained. Only 40.8 and 27.1 % adsorption was observed within 2 h whereas the final color removal efficiencies were found to be 94.1 and 79.8 % within 28 and 31 h, respectively. Although the final color removal efficiency at initial congo red concentrations of 20 and 50 mg L^{-1} showed no significant differences, the equilibrium time between the solutions differed by 25 h. These results may be explained by the following: A large number of vacant surface sites are available for adsorption during the initial stage of adsorption or under low initial congo red concentration. With increasing adsorption time, the remaining vacant surface sites became difficult to occupy due to repulsive forces between the congo red dye adsorbed on the surface of the magnetic *Rhizopus oryzae* biomass particles and solution phase[40]. The amount of congo red adsorbed per unit weight of magnetic *Rhizopus oryzae* biomass particles at equilibrium increased with increasing initial congo red concentration. As the initial concentration increased from 5 to 80 mg L^{-1}, the equilibrium adsorption capacity increased from 6.32 to 65.19 mg g^{-1}. Therefore, the adsorption process is highly dependent on the initial congo red concentration and contact time.

Adsorption kinetics: To further expose the adsorption mechanism of congo red onto magnetic *Rhizopus oryzae* biomass particles rate-controlling steps, a kinetic investigation was conducted. The Lagergren-first-order, pseudo-second-order and intra-particle diffusion kinetic models were applied to model the kinetics of congo red adsorption onto magnetic *Rhizopus oryzae* biomass particles.

Lagergren-first-order kinetic model[41] is generally expressed as:

$$\log (q_e - q_t) = \log q_e - \frac{k_1 t}{2.303} \quad (3)$$

where q_e and q_t are amounts of congo red (mg g^{-1}) adsorbed on the adsorbent at equilibrium and at a given time t, respectively and k_1 is the rate constant (min^{-1}) of the adsorption model, the value of which can be calculated from plots of log (q_e-q_t) versus t as in eqn. 3.

The pseudo-second-order kinetic model[42] proposed by Ho and McKay is expressed as follows:

$$\frac{t}{q_t} = \frac{1}{k_2 q_e^2} + \frac{t}{q_e} \quad (4)$$

where k_2 is the rate constant (g mg^{-1} min^{-1}) of the pseudo-second-order kinetic model of adsorption. By plotting a curve of t/q_t against t, q_e and k_2 can be evaluated. The adsorption parameters were determined at different initial congo red concentrations. Results are presented in Fig. 8a,b and Table-1.

In all studied initial congo red concentrations, extremely high correlation coefficients (> 0.991) were obtained from calculations using the pseudo-second order kinetic equation. In addition, calculated q_e values were also in agreement with the experimental data in the case of pseudo-second-order kinetics

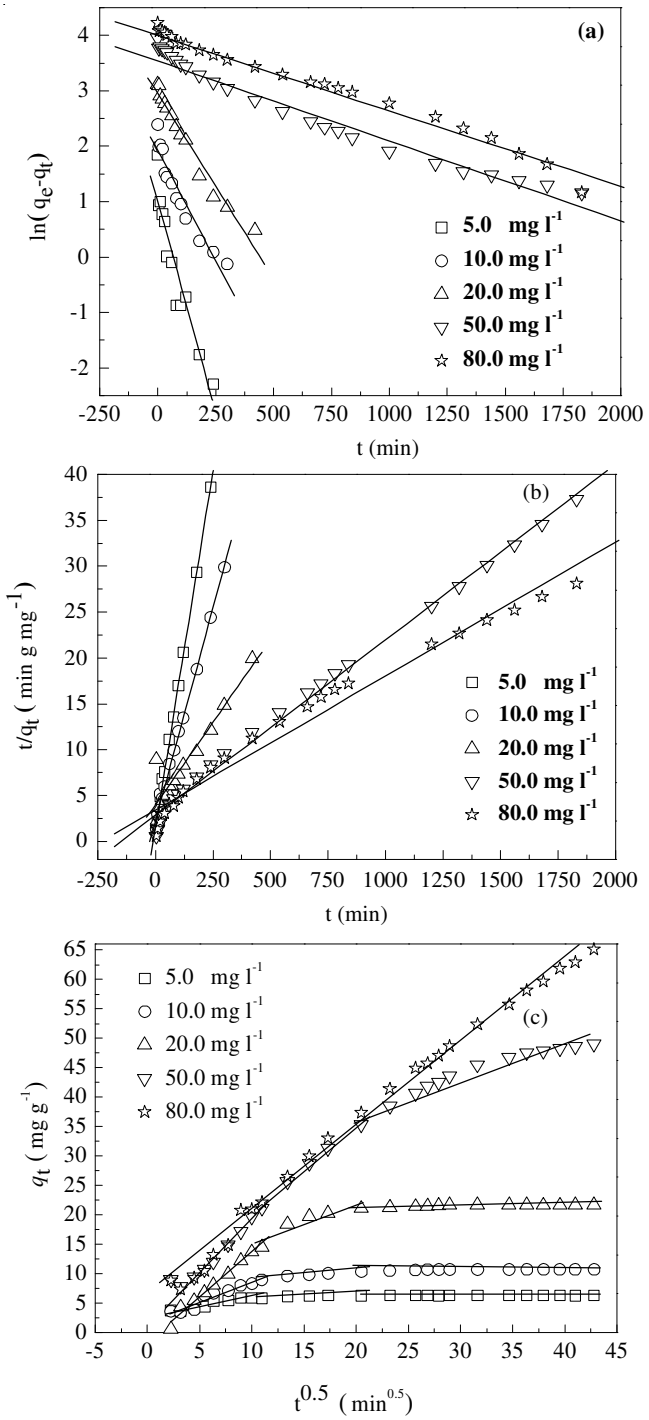

Fig. 8. Linear regressions of kinetics plot: (a) lagergren-first-order model, (b) pseudo-second-order model and (c) Intra-particle diffusion model

when the congo red concentration ranged from 5 to 50 mg L^{-1}, implying that the adsorption process completely follows pseudo-second order kinetics at low congo red concentrations. With the congo red concentration increased (80 mg L^{-1}), the correlation coefficients (R^2) of pseudo-first order model reached 0.996, higher than that of pseudo-second-order model (0.991). Moreover, $q_{e,cal}$ (63.92 mg g^{-1}) was very close to $q_{e,exp}$ (65.19 mg g^{-1}). The pseudo-second-order model is based on the assumption that the rate-determining step may be chemical sorption involving valence forces through the sharing or exchanging of electrons between the adsorbent and sorbate.

For example, chitin has two main functional groups, the hydroxyl and amino groups, per glucosamine unit. Therefore, the dye could be adsorbed by interaction between the congo red dye molecules and the functional groups of chitin in magnetic *Rhizopus oryzae* biomass particles at low congo red concentrations. The Lagergren-first-order kinetic model indicates that the rate of occupation of biosorption sites is proportional to the number of unoccupied sites. Congo red dye molecules compete with each other for the active surface sites of magnetic *Rhizopus oryzae* biomass particles at high congo red concentrations (80.0 mg L^{-1}) and the chemical interaction involving valence forces between the adsorbent and sorbate became is weakened[20,34].

To assess the nature of the diffusion process, kinetic data were analyzed using an intra-particle diffusion model[25] to elucidate the diffusion mechanism:

$$q_t = k_i t^{1/2} + c \quad (5)$$

where c (mg g^{-1}) is the intercept and k_i is the intra-particle diffusion rate constant (mg g^{-1} $min^{-1/2}$). The value of ki can be calculated from the slop of linear plots of qt versus $t^{1/2}$.

Prediction of the rate-limiting step in an adsorption process is very important to understand the sorption mechanism of the particles. According to this model, if the plot of q_t versus $t^{1/2}$ gives a straight line, then the adsorption process is controlled by intra-particle diffusion. If the data exhibit multilinear plots, then two or more steps influence the adsorption process[35]. All of the correlation coefficients for the intra-particle diffusion model were lower than those of the pseudo-first-order and the pseudo-second-order models when the congo red concentration was within 5 to 50 mg L^{-1}, as shown in Fig. 8c and Table-2.

This result indicates that congo red adsorption onto magnetic *Rhizopus oryzae* biomass particles does not follow the intra-particle diffusion kinetics. Plots of q_t *versus* $t^{1/2}$ can be divided into a multi-linearity correlation (Fig. 8c), indicating the occurrence of three steps during adsorption process at low congo red concentration. Congo red in aqueous solution is first transported onto the surface of magnetic *Rhizopus oryzae* biomass particles (film diffusion). The second step is the gradual adsorption stage, where intra-particle diffusion with k_2 (0.053, 0.144, 0.765 and 1.515 mg g^{-1} $min^{-1/2}$ for 5, 10, 20 and 50 mg L^{-1}, respectively) can be rate-controlling. The third step is the final equilibrium stage, where intra-particle diffusion starts to slow down due to the extremely low solute concentration in the solution. In the intermediate stage, where adsorption is gradual, the process may be controlled by intra-particle diffusion, indicating that intra-particle diffusion is involved in congo red adsorption onto magnetic *Rhizopus oryzae* biomass particles, but is not the sole rate-controlling-step. The plot of q_t versus $t^{1/2}$ gives a straight line at increased congo red concentration (80 mg L^{-1}), indicating that the adsorption process is only controlled by intra-particle diffusion. From the above analysis, film diffusion and intra-particle diffusion simultaneously operate during congo red adsorption on magnetic *Rhizopus oryzae* biomass particles at low concentration (5-50 mg L^{-1}) and are enhanced with increasing initial congo red concentration. Intra-particle diffusion is the sole rate-limiting step at high congo red concentration (80 mgL^{-1}).

Equilibrium adsorption isotherm: The Langmuir and Freundlich isotherm models were used to describe the equilibrium adsorption of congo red on magnetic *Rhizopus oryzae* biomass particles. Linear forms of the Langmuir equation[43] eqn. 6 and Freundlich isotherm[44] eqn. 7 after rearrangement are as follows:

$$\mathrm{Ln}q_e = \mathrm{Ln}K_F + \frac{1}{n}\mathrm{Ln}C_e \quad (6)$$

$$\frac{C_e}{q_e} = \frac{C_e}{q_m} + \frac{1}{K_L q_m} \quad (7)$$

where q_e (mg g^{-L}) is the adsorption capacity of congo red adsorbed at equilibrium, Ce(mg L^{-1}) is the equilibrium concentration of congo red in solution. q_m (mg g^{-1}) is the maximum amounts of congo red adsorbed per unit weight of adsorbent required for monolayer coverage of the surface, K_L(L

TABLE-1
A COMPARISON OF LAGERGREN-FIRST-ORDER MODEL AND PSEUDO-SECOND-ORDER MODEL RATE CONSTANTS CALCULATED FROM EXPERIMENTAL DATA

C_0(mg l^{-1})	$q_{e,exp}$ (mg g^{-1})	Lagergren-first-order kinetic model			Pseudo-second-order kinetic model		
		$q_{e,cal}$(mg $g^{?1}$)	k_1(min^{-1})	R^2	$q_{e,cal}$(mg $g^{?1}$)	K_2(min^{-1})	R^2
5.0	6.32	2.79	0.0357	0.950	6.31	0.02562	1.000
10.0	10.88	6.86	0.0183	0.954	10.92	0.00382	1.000
20.0	21.75	19.12	0.0154	0.982	22.71	0.00070	0.999
50.0	49.13	43.05	0.0035	0.984	52.22	0.00013	0.997
80.0	65.19	63.92	0.0033	0.996	68.31	0.00006	0.991

TABLE-2
INTRA-PARTICLE DIFFUSION MODEL FOR CONGO RED ADSORPTION ON MAGNETIC *Rhizopus oryzae* BIOMASS PARTICLES FOR DIFFERENT INITIAL CONCENTRATIONS

C_0(mg l^{-1})	Whole process			First stage			Second stage			Third stage		
	C (mg $g^{?1}$)	k_i (mg $g^{?1}$ $min^{?0.5}$)	R^2	C_1 (mg $g^{?1}$)	K1(mg $g^{?1}$ $min^{?0.5}$)	R_1^2	C_2 (mg $g^{?1}$)	K_2(mg $g^{?1}$ $min^{?0.5}$)	R_2^2	C_3 (mg $g^{?1}$)	K_3(mg $g^{?1}$ $min^{?0.5}$)	R_3^2
5.0	4.799	0.047	0.727	2.926	0.295	0.953	5.392	0.053	0.983	6.28	2.0×10^{-5}	1.000
10.0	5.826	0.151	0.823	2.069	0.646	0.934	7.498	0.144	0.97	10.273	0.0123	0.999
20.0	7.425	0.437	0.850	1.133	1.454	0.998	6.500	0.764	0.96	20.878	0.0206	0.999
50.0	8.203	1.107	0.974	0.544	1.876	0.997	4.830	1.515	0.997	27.07	0.538	0.980
80.0	5.464	1.458	0.996	–	–	–	–	–	–	–	–	–

mg^{-1}) is a constant related to the heat of adsorption. $K_F(mg^{1-(1/n)}L^{1/n}g^{-1})$ is related to the adsorption capacity of the adsorbent and 1/n is another constant related to the surface herogeneity. The theoretical parameters (q_m, K_L, K_F and n and R^2) of the adsorption isotherms are summarized in Table-3.

TABLE-3
ISOTHERM MODELS CONSTANTS AND REGRESSION COEFFICIENTS FOR CONGO RED ADSORPTION ONTO MAGNETIC *Rhizopus oryzae* BIOMASS PARTICLES

T(K)	Langmuir isotherm constants			Freundlich isotherm constants		
	q_m (mg g^{-1})	K_L	R^2	K_F ($mg^{1-(1/n)}l^{1/n}g^{-1}$)	n	R^2
298	69.78	0.85	0.994	24.78	2.92	0.955

Congo red adsorption on magnetic *Rhizopus oryzae* biomass particles fits the Langmuir model (R^2 = 0.994) better than the Freundlich model (R^2 = 0.955) under the concentration range studied due to the homogeneous distribution of active sites on the magnetic *Rhizopus oryzae* biomass particles surface, since the Langmuir equation assumes a homogenous surface. As seen in Table-3, the maximum adsorption capacity of congo red onto magnetic *Rhizopus oryzae* biomass particles is 69.78 mg g^{-1}, consistent with the experimentally obtained value and indicating a monolayer adsorption process.

Conclusion

In this study, magnetic *Rhizopus oryzae* biomass particles were synthesized and characterized as a novel adsorbent for the removal of typical azo dye (CR) from aqueous solution. The adsorbent dose, initial congo red concentration and contact time during adsorption played significant roles in the dye adsorption capacity of magnetic *Rhizopus oryzae* biomass particles. In the kinetic study, the pseudo-second order kinetic model described the process of congo red adsorption on magnetic *Rhizopus oryzae* biomass particles at low congo red concentration (5-50 mg L^{-1}) very well. Adsorption kinetic studies also revealed that three stages in the adsorption process. Both film diffusion and intra-particle diffusion simultaneously operated during adsorption at low congo red concentrations (5-50 mg L^{-1}). Intra-particle diffusion is the sole rate-limiting step at high congo red concentration (80 mg L^{-1}). Isotherm modeling revealed that the Langmuir equation could better describe congo red adsorption on magnetic *Rhizopus oryzae* biomass particles compared with Freundlich models. Batch adsorption experiments showed that magnetic *Rhizopus oryzae* biomass particles may have broad applications in the removal of anionic azo dyes from wastewater and that it can be competitive with conventional adsorbents. Other studies on this bioadsorbent continue in our laboratory and more detailed results will appear in a forthcoming paper.

ACKNOWLEDGEMENTS

This work was financially supported by the National Natural Science Foundation of China (Grant Nos. 21106091. 51208331) and Zhejiang Provincial Natural Science Foundation of China (LQ12B06004).

REFERENCES

1. G. Crini, *Bioresour. Technol*., **97**, 1061 (2006).
2. H. Park and W. Choi, *J. Photochem. Photobiol. Chem*., **159**, 241 (2003).
3. R. Gong, Y. Ding, M. Li, C. Yang, H. Liu and Y. Sun, *Dyes Pigments*, **64**, 187 (2005).
4. K.C. Chen, J.Y. Wu, C.C. Huang, Y.M. Liang and S.C.J. Hwang, *J. Biotechnol*., **101**, 241 (2003).
5. M.S. Chiou and G.S. Chuang, *Chemosphere*, **62**, 731 (2006).
6. S. Chinwetkitvanich, M. Tuntoolvest and T. Panswad, *Water Res*., **34**, 2223 (2000).
7. U. Mayer, *FEMS Symp*., **12**, 371-385 (1981).
8. K.T. Chung and C.E. Cerniglia, *Mutat. Res*., **277**, 201 (1992).
9. G. Ciardelli, L. Corsi and M. Marcucci, *Resour. Conserv. Recycling*, **31**, 189 (2001).
10. K. Swaminathan, S. Sandhya, A. Carmalin Sophia, K. Pachhade and Y.V. Subrahmanyam, *Chemosphere*, **50**, 619 (2003).
11. I.D. Mall, V.C. Srivastava, N.K. Agarwal and I.M. Mishra, *Chemosphere*, **61**, 492 (2005).
12. C. Namasivayam and D.J.S.E. Arasi, *Chemosphere*, **34**, 401 (1997).
13. L. Wang and A.Q. Wang, *J. Chem. Technol. Biotechnol*., **82**, 711 (2007).
14. P.R. Austin, C.J. Brine, J.E. Castle and J.P. Zikakis, *Science*, **212**, 749 (1981).
15. M.K. Jang, B.G. Kong, Y.I. Jeong, C.H. Lee and J.W. Nah, *J. Polym. Sci. Pol. Chem*., **42**, 3423 (2004).
16. U. Filipkowska, *Environ. Technol*., **29**, 681 (2008).
17. Y. Shimizu, K. Kono, I.S. Kim and T. Takagishi, *J. Appl. Biomater*., **5**, 245 (1995).
18. C.Y. Kim, H.M. Choi and H.T. Cho, *J. Appl. Polym. Sci*., **63**, 725 (1997).
19. W. Liao, Y. Liu, C. Frear and S.L. Chen, *Bioresour. Technol*., **99**, 5859 (2008).
20. L. Mogollón, R. Rodríguez, W. Larrota, N. Ramirez and R. Torres, *Appl. Biochem. Biotechnol*., **70-72**, 593 (1998).
21. C.J. Banks and M.E. Parkinson, *J. Chem. Technol. Biotechnol*., **54**, 192 (1992).
22. Y. Fu and T. Viraraghavan, *Water Qual. Res. J. Canada*, **35**, 95 (2000).
23. E. Fourest and J.C. Roux, *Appl. Microbiol. Biotechnol*., **37**, 399 (1992).
24. Y. Sag and T. Kutsal, *Process Biochem*., **33**, 571 (1998).
25. H.Y. Zhu, R. Jiang, L. Xiao and G.M. Zeng, *Bioresour. Technol*., **101**, 5063 (2010).
26. H.Y. Zhu, R. Jiang and L. Xiao, *Appl. Clay Sci*., **48**, 522 (2010).
27. M. Šafaríková and I. Šafarík, *Biotechnol. Lett*., **22**, 941 (2000).
28. G.Y. Li, Y.R. Jiang, K.L. Huang, P. Ding and J. Chen, *J. Alloys Compd*., **466**, 451 (2008).
29. M. Šafaríková, L. Ptácková, I. Kibriková and I. Šafarík, *Chemosphere*, **59**, 831 (2005).
30. I. Šafarík, L.F.T. Rego, M. Borovská, E. Mosiniewicz-Szablewska, F. Weyda and M. Šafaríková, *Enzyme Microb. Technol*., **40**, 1551 (2007).
31. I.C. Mac Rae, *Water Res*., **20**, 1149 (1986).
32. G.R. Mudasir, I. Tahir and E.T. Wahyuni, *J. Phys. Sci*., **19**, 63 (2008).
33. L. Wang and A.Q. Wang, *Chem. Eng. J*., **143**, 43 (2008).
34. H.Y. Zhu, Y.Q. Fu, R. Jiang, J.H. Jiang, L. Xiao, G.M. Zeng, S.L. Zhao and Y. Wang, *Chem. Eng. J*., **173**, 494 (2011).
35. H. Chen, G.L. Dai, J. Zhao, A.G. Zhong, J.Y. Wu and H. Yan, *J. Hazard. Mater*., **177**, 228 (2010).
36. S. Chatterjee, S.K. Das, R. Chakravarty, A. Chakrabarti, S. Ghosh and A.K. Guha, *J. Hazard. Mater*., **174**, 47 (2010).
37. Q.Q. Peng, Y.Q. Liu, G.M. Zeng, W.H. Xu, C.P. Yang and J.J. Zhang, *J. Hazard. Mater*., **177**, 676 (2010).
38. A. Sari, M. Tuzen, D. Citak and M. Soylak, *J. Hazard. Mater*., **149**, 283 (2007).
39. G.Vijayakumar, M. Dharmendirakumar, S. Renganathan, S. Sivanesan, G. Baskar and K.P. Elango, *Clean*, **37**, 355 (2004).
40. S. Senthilkumaar, P.R. Varadarajan, K. Porkodi and C.V. Subbhuraam, *J. Colloid Interface Sci*., **284**, 78 (2005).
41. Y. Qu, C. Zhang, F. Li, X. Bo, G. Liu and Q. Zhou, *J. Hazard. Mater*., **169**, 146 (2009).
42. M.Y. Arica and G. Bayramoglu, *J. Hazard. Mater*., **149**, 499 (2007).
43. I. Langmuir, *J. Am. Chem. Soc*., **40**, 1361 (1918).
44. H.M.F. Freundlich, *Z. Phys. Chem*., **A57**, 358 (1906).